Petroleum Science 19 (2022) 1007–1018

Contents lists available at ScienceDirect

Petroleum Science

journal homepage: www.keaipublishing.com/en/journals/petroleum-science

Original Paper

Investigation of oil and water migrations in lacustrine oil shales using 20 MHz 2D NMR relaxometry techniques

Bo Liu [b], Xiao-Wen Jiang [a, c], Long-Hui Bai [b], Rong-Sheng Lu [a, c, d, *]

[a] Jiangsu Key Laboratory for Design and Manufacture of Micro-Nano Biomedical Instruments, Southeast University, Nanjing, Jiangsu 211189, China
[b] State Key Laboratory Cultivation Base for Accumulation and Development of Unconventional Oil and Gas, Northeast Petroleum University, Daqing, Heilongjiang 163318, China
[c] School of Mechanical Engineering, Southeast University, Nanjing, Jiangsu 211189, China
[d] State Key Laboratory of Bioelectronics, Southeast University, Nanjing, Jiangsu 211189, China

ARTICLE INFO

Article history:
Received 27 July 2020
Accepted 15 July 2021
Available online 23 October 2021

Edited by Jie Hao

Keywords:
NMR Relaxometry
Lacustrine oil shales
Oil and water migrations
T_1-T_2 map

ABSTRACT

The behavior of oil and water in tight rocks can change the distribution of oil or water in pores, which affects the production of crude oil. Nuclear Magnetic Resonance (NMR) method is an effective and non-destructive tool for evaluating rocks with comparison and analysis both quantitatively and qualitatively. In our study, 20 MHz NMR Relaxometry is used as a key technique to study the changes of water and oil behaviors in Chinese lacustrine Qingshankou shales under different saturated states (imbibition and evaporation without pressure). The results show that variation in different proton populations (water, oil and organic) can be distinguished using 2D T_1–T_2 maps. The comparison among T_1-T_2 maps with different saturated states shows that different signal regions changed during oil and water migrations, which the 1D NMR Relaxometry may be not easy to approach. Combined with the pyrolysis analysis, T_2 shift and differences of signal regions in T_1-T_2 maps can reflect properties such as wettability and composition (organic matter, clay and magnetic minerals) to some extent. This study provides better insight into oil and water behaviors in lacustrine oil shales with further understanding of 20 MHz NMR 2D T_1-T_2 maps both in qualitative and quantitative analysis.

1. Introduction

The migrations of oil and water molecules in pores of shale reservoir are very complex. These behaviors can be affected not only by temperature and capillary pressure, but also by the interaction between molecules and pore surface. Besides, the saturation of liquid in tight rocks may also make much difference. Therefore, understanding how and why the oil and water molecules move in shales can be a helpful way to study the petrophysical properties such as pore-size distribution, wettability and liquid saturation of rocks. Furthermore, these characteristics are all important for evaluating the difficulty of crude oil collection so that can bring great economic benefits. Thus, it is essential to catch the migrations of oil and water in shales under different saturated conditions. However, conventional experimental means such as Dean-Startk analysis (McPhee et al., 2015) and Rock-Eval pyrolysis (Baudin et al., 2015) have their own limits and can hardly investigate tight rocks with no destruction.

Nuclear Magnetic Resonance (NMR) has become a common method both in well logging (Coates et al., 1999; Xie and Xiao, 2011; Liao et al., 2021) and core samples analysis (Ramia and Martín, 2016) for its non-invasive and non-destructive nature. The structure and composition of core samples can truly affect the longitudinal (T_1) and transverse (T_2) relaxation mechanisms, which are two prime relaxation mechanisms in NMR experiments. According to the so-called Bloembergen-Purcell-Pound theory (BPP theory) (Bloembergen et al., 1948), the T_1 and T_2 relaxation constants of a pure fluid are related to its condition, in consideration of molecular motion. So that NMR can distinguish the fluid type such as free water, bounded water and oil (Shi et al., 2019; Deng et al., 2020; Zhong et al., 2020). As for fluid in confinement or in pores, the theory of biphasic fast-exchange relations (Kleinberg et al., 1994; Godefroy et al., 2001; Korb, 2018) is used to obtain pore size

* Corresponding author. Jiangsu key laboratory for Design and Manufacture of Micro-Nano Biomedical Instruments, Southeast University, Nanjing, 21189, China.
E-mail address: lurs@seu.edu.cn (R.-S. Lu).

https://doi.org/10.1016/j.petsci.2021.10.011

distribution, in correspondence with T_1 and T_2 distribution. It is why NMR technique is a powerful tool to investigate petrophysical properties of conventional rocks such as fluid saturation and typing (Testamanti and Rezaee, 2017; Liu et al., 2018), porosity (Blümich et al., 2004) and pore size distribution (Gao et al., 2018; Guo et al., 2020; Wang et al., 2020). Besides, 2-dimensional NMR (2D NMR) Relaxometry (Korb et al., 2014; Fleury and Romero-Sarmiento, 2016) taking advantage of T_1/T_2 ratios is an effective tool that can identify water, oil, and solid organics in shale samples both quantitatively and qualitatively (Khatibi et al., 2019). Some researchers also used 2D NMR to characterize wettability, permeability or pores connectivity of rocks and got some preliminary experimental results (Fan et al., 2018; Liang et al., 2019; Tian, 2021).

For unconventional shale oil reservoirs, their low permeability and complex components extremely increase the difficulty of NMR analysis. Usually, low-field NMR measurement with 2 MHz is insufficient to meet the requirements of resolution. In recent years, higher field NMR measurement with 22 MHz is proposed to analyze unconventional rocks (Liu et al., 2019a; Xie and Gan, 2019). Compared with 2 MHz NMR, 22 MHz NMR can not only bring attractive profits in signal-to-noise ratio (SNR), saving the detection time with fewer scan times, but also capabilities to measure bound water and solid organics with very short T_2 relaxation time (Xie and Gan, 2018).

In this paper, we used 20 MHz 2D NMR Relaxometry as a key technique to investigate water and oil behaviors of Chinese lacustrine Qingshankou shales in the Songliao Basin. A quantitative method of hydrogen content using NMR T_1-T_2 maps was introduced. Compared with samples weight measured by a balance, NMR signals demonstrated the accuracy of 20 MHz 2D NMR Relaxometry technique. NMR T_1-T_2 maps with a pixel matrix of 181×181 were measured to analyze the changes of shales under different saturated conditions, for example, oil imbibed condition and brine imbibed condition. The result details were discussed to illustrate NMR responses corresponding to the various components in source rock samples. This study shows how NMR signal changes in the tight pore system during imbibition and evaporation, and allows us to forward in understanding the effects of water and oil on the physical parameters of petroleum in shales. It also shows the potential of 20 MHz 2D NMR Relaxometry to be a useful probe to access the characterization of dynamics in unconventional shale rocks.

2. Samples and methodology

2.1. Samples

In this study, three chunks of shale samples of different depths in a well were selected from the first member of Qingshankou (abbreviated as Q1) Formation in central depression, northern Songliao Basin as shown in Fig. 1a. The Songliao Basin as well as Hailar Basin are the largest two oil-bearing basins in northeast China (Liu et al. 2019b, 2020). Normally, the Songliao Basin would be divided into six first-order tectonic units, namely northern plunge, western slope, southwestern uplift, southeastern uplift, northeastern uplift, and central depression. For this study, the location of sampling well is shown in Fig. 2b. The Qingshankou Formation is divided into three members, Q1, Q2 and Q3 from bottom to top. And the Q1 Formation is dominated by lacustrine expansion and organic matter rich continental shale formed in lacustrine expansion. Besides, the shale within the Q1 Formation is oil prone and mainly in the oil window, which makes it one of the main shale oil targets in China (Liu et al., 2020).

The Q1 Formation of sampling well has high organic abundance and the total organic carbon (TOC) ranges from 0.5 wt% to 4.0 wt%, with an average of TOC >2.0 wt%. The hydrogen index (HI) obtained from Rock-Eval measurements ranges from 300 mg/g to 800 mg/g, with most of HI > 440 mg/g. The organic matter is in the moderate maturity and the T_{max} ranged from 430 °C to 460 °C, with most of T_{max} > 430 °C. The minerals are mainly composed of quartz and clay minerals, followed by feldspar and calcite. Pyrite and siderite are common. The content of quartz ranges from 20 wt% to 45 wt%, with most of content >35 wt%, and the content of clay minerals ranges from 10 wt% to 45 wt%, with most of content >30 wt% (Liu et al. 2017, 2019b).

2.2. Bulk geochemical parameters and mineral composition measurement

To obtain the TOC content, inorganic carbon was stripped away from shale samples by using dilute hydrochloric acid. Organic carbon in the sample was then converted to CO_2 by burning the sample in a high-temperature oxygen stream using a CS-230 analyzer, and TOC value was determined by using an infrared detector. Geochemical parameters were measured by using Rock-Eval including S_1, S_2 and T_{max}. S_1 is the sample residual hydrocarbon content and S_2 is pyrolysis hydrocarbon content. T_{max} represents a good correlation with the maturity of the source rock. The hydrogen index (HI) and the oil saturation index (OSI) were calculated by using S_1, S_2 and TOC value ($HI = S_2/TOC \times 100$, $OSI = S_1/TOC \times 100$). X-ray diffraction (XRD) is a powerful and rapid analytical technique method for characterizing materials in shales. The mineral compositions of the shale samples selected were measured by the D/max-2200-Xray diffractometer. Surface properties of the shale samples were characterized by using Scanning Electron Microscopy (SEM) (FEI, Quanta450FEG).

2.3. Imbibition and evaporation procedures

Oil imbibition and brine imbibition in ambient temperature were adopted to change saturated states of shale samples, which could cause nearly no harm compared with saturation under pressure. Each chunk of shale sample was divided into two portions—one was used for oil (decane) imbibition and the other was used for brine (8000 ppm $NaHCO_3$ solution) imbibition. Brine was set up to provide shale with a liquid environment like that in mine. Decane and $NaHCO_3$ were supplied by Beyond Industries (China) Limited.

The specific operation steps of the imbibition experiment were as follows. Every chunk of shale samples was divided into two portions. Two portions of the original shale sample were placed in two beakers covered with a thin layer of decane or brine, respectively. The liquid level height in the container was then increased every 8 h until the shale sample was fully immersed in liquid. The liquid volume added each time was about 5 mm′s tall, not very precisely. Five or six times were enough to make sure that the shale sample was fully immersed. It should be noticed that imbibition is a displacement due to capillary forces and it is a very slow process that may take up to several days to finish.

To study the changes of shales during the oil imbibition and brine imbibition process, two portions of a chunk of shale sample (from 2107.59 m depth) were under oil and brine imbibition process for up to three weeks, respectively. The shale samples were taken out of beakers for NMR T_1-T_2 map measurement after each certain period (2 days, 5 days, 14 days, 21 days). After three weeks, the two portions were dried in an oven at 60 °C for 24 h. Every 6 h, the shale samples were taken out of oven, cooled to lab temperature and measured by NMR analyzer. Another two chunks of shale samples (from 2088.99 m to 2138.60 m depth) were under imbibition process for 60 h to compare their wettability. All imbibition experiments were done at ambient condition. After oil or brine

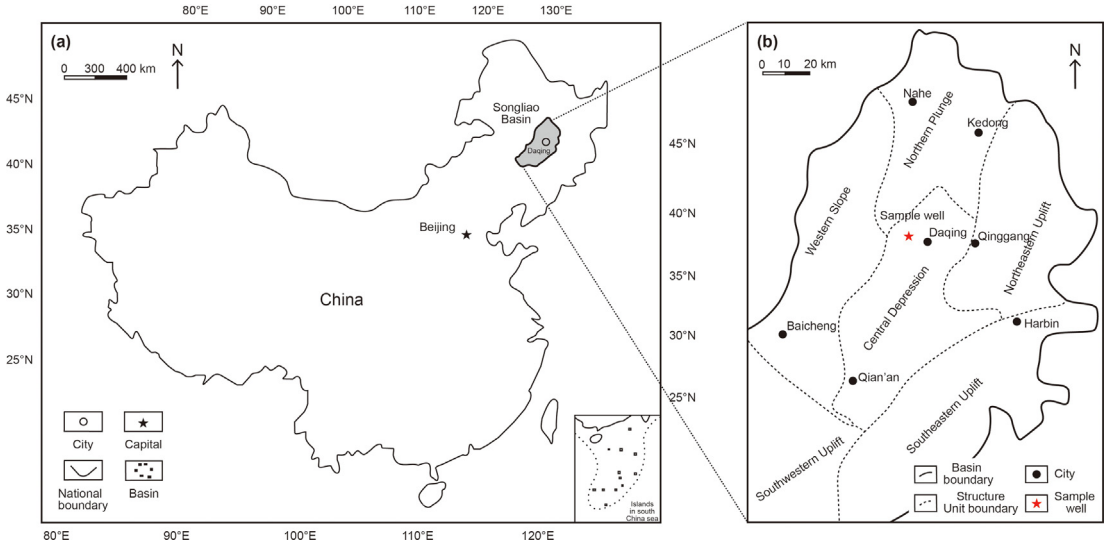

Fig. 1. (a) Location along with six tectonic units maps of the Songliao Basin. (b) The study area. (modified from Liu et al., 2019b).

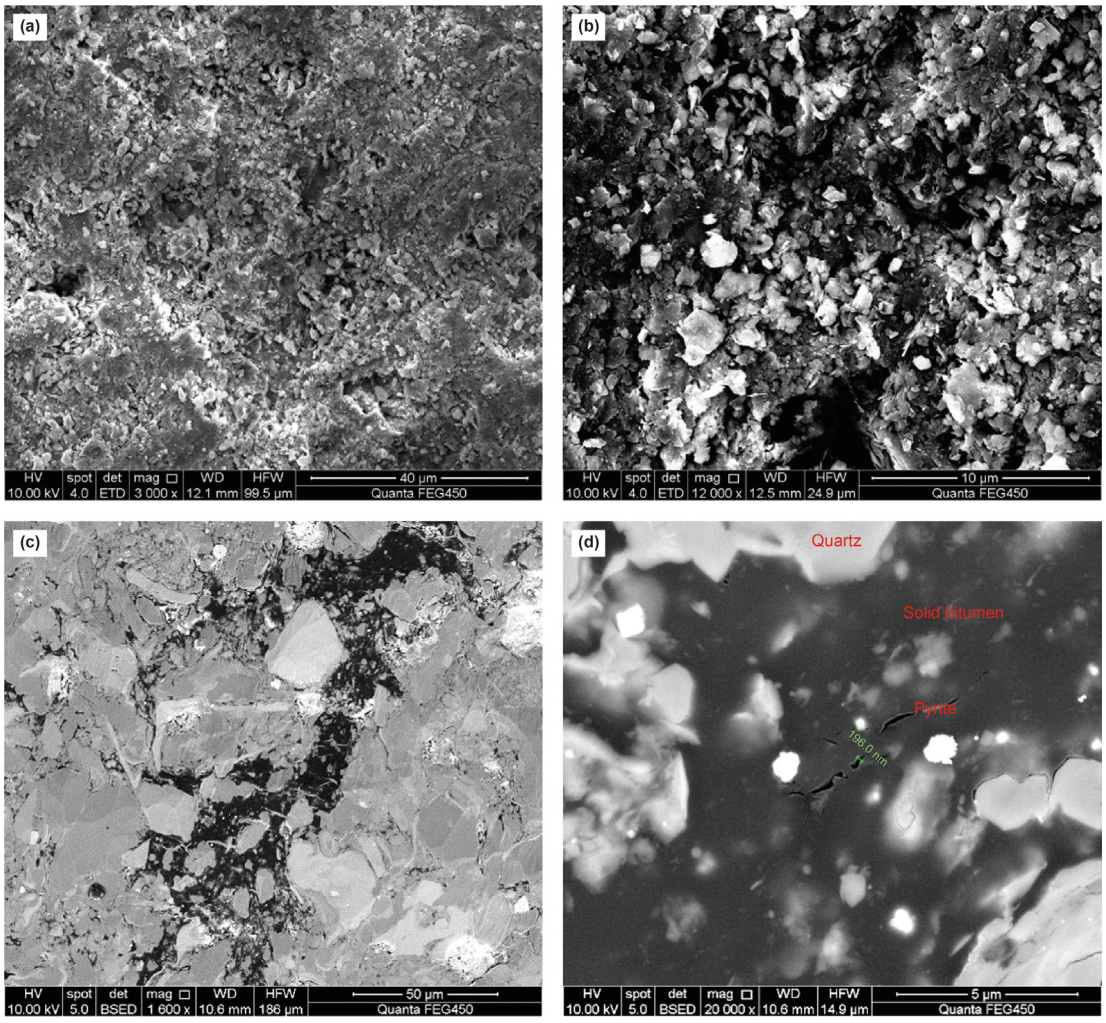

Fig. 2. Surface properties of shale samples characterized by SEM: (a) SEs detector, marker = 20 μm; (b) SEs detector, marker = 10 μm; (c) BSEs detector, maker = 50 μm; (d) BSEs detector, marker = 5 μm.

imbibition, all imbibed shale samples were finally dried in an oven at 60 °C for 24 h. Considering the increase in weight that should come entirely from the changes of oil or brine in samples, samples were carefully weighed before and after imbibition or evaporation.

2.4. NMR T_1-T_2 map experiment

NMR T_1-T_2 mapping experiments were carried out on the samples at each stage using a 20 MHz MR Cores (Houston, USA), equipped with a 30 mm probe optimized for unconventional shales experiments. The short ring down delay time (also called dead time) which is related to the NMR probe and NMR electronic control system is less than 15 μs to allow for the capture of fast-decaying relaxation signals in tight rocks.

NMR T_1-T_2 correlation data were acquired using T_1-T_2 pulse sequence, a pulse sequence combining the Inversion Recovery (IR) sequence and Carr-Purcell-Meiboom-Gill (CPMG) sequence, where the signal amplitude was determined from the first CPMG echo. The echo spacing time (TE) was 0.06 ms with no less than 2000 echo points and the T_1 weighted delays were from 0.1 ms to 2.5 s with 64 steps by equal logarithm interval. The number of scan times was 16 for imbibed samples or 32 for dried samples to ensure an adequate signal-to-noise ratio (SNR) that was no less than 1000. Repetition time (TR) between each scan was set up to 5 s and the detection time of each shale was no less than 6 h.

T_1-T_2 maps were derived from NMR T_1-T_2 correlation date to obtain T_1-T_2 2-D distribution using an Optimized Truncated Singular Value Decomposition (OTSVD) inversion method. The pixel matrix setting of all T_1-T_2 maps was 181 × 181, considering the operation speed and imaging resolution comprehensively.

2.5. NMR signal calibration

Amplitude of NMR signal is very sensitive and proportional to the hydrogen content in a sample. In our experiments, all NMR signals were calibrated in hydrogen content unit, mg, by using a standard liquid sample (1% $CuSO_4$ solution). The standard liquid sample with a known hydrogen content (585.556 mg) was completely sealed, so its hydrogen content was always the same during the experiment. Every time the T_1-T_2 map of a shale sample was measured, the T_1-T_2 map of the standard liquid sample was detected to eliminate the error caused by the instrument in different time periods as well. The hydrogen content of the shale sample was calculated according to the ratio of NMR signal amplitude of the shale sample and the standard liquid sample.

3. Results

3.1. Geochemical characteristics and mineral composition

The results of TOC content and Rock-Eval pyrolysis are shown in Table 1. These samples had OSI values exceeding to 100 mg/g, showing good shale oil potential. The TOC content was not high and not much different among the three shale samples. The results of mineral composition measured by XRD are shown in Table 2, which shows that the clay content could not be neglected and the differences were also not significant among the three shale samples. Magnetic mineral components such as siderite and pyrite did exist in these shale samples and the total content was tolerable. Scanning electron microscope (SEM) images of shale samples obtained by secondary electrons (SEs) detector and backscattered electrons (BSEs) detector are shown in Fig. 2.

3.2. Changes of sample weight and hydrogen content during imbibition and evaporation

The weight of three shale samples at different stages is shown in Table 3. Each shale sample had two portions, one for oil imbibition and the other for brine imbibition. Each portion of shale samples experienced three stages, i.e. native, imbibed and dried. Native condition denotes that the shale sample was fresh “as received”. Imbibed condition denotes that the shale sample was oil imbibed (for oil portion) or brine imbibed (for brine portion) after imbibition process. Dried condition denotes that the imbibed shale sample in the previous stage was dried after evaporation.

Hydrogen content of these three shale samples increased in imbibed condition and decreased after drying process. There were some differences between the shale sample (from 2107.59 m depth) under three-week imbibition and the other two shale samples (from 2088.99 m depth and 2138.60 m depth) under 60-h imbibition. Obviously, for the shale sample from 2107.59 m, the hydrogen content in oil portion and brine portion of dried condition was slightly higher than that of native condition. And for the shale samples from 2088.99 m to 2138.60 m depth, the hydrogen content in brine portion of dried condition was lower than that in native condition. But hydrogen content in oil portion of dried condition was still a little bit higher than that in native condition.

Hydrogen content measured by NMR 2D mapping of the shale sample from 2107.59 m depth, which changed with sample weight during imbibition and evaporation process, is shown in Table 4 and Fig. 3. NMR signal or the hydrogen content measured by NMR 2D mapping had a good linear relationship with the sample weight. The results of linear regression, R-squared, were 0.984 (Figs. 3a) and 0.988 (Fig. 3b) respectively. The slop of fitted straight line in Fig. 3a was about 172.05 mg/g, which was a little bit larger than 154.92 mg/g, the hydrogen content of decane ($C_{10}H_{22}$). And the slop in Fig. 3b was about 108.63 mg/g, which was very close to 111.11 mg/g, the hydrogen content of water (H_2O).

3.3. Oil and water migrations in NMR T_1-T_2 maps

Fig. 4 shows NMR T_1-T_2 maps of the shale sample from 2107.59 m depth at different imbibed stages of 0 days (native), 5

Table 1
Bulk geochemical parameters of three selected shale samples.

Depth, m	S_1, mg/g	S_2, mg/g	T_{max}, °C	TOC, %	HI, mg/g	OSI, mg/g	PI	Type of kerogen
2107.59	3.544	8.774	444.3	2.55	344.39	139.11	0.29	II_1
2088.99	4.494	15.277	505.6	3.07	498.13	146.53	0.23	II_1
2138.60	8.054	11.781	449.1	2.01	587.47	401.62	0.41	I

Table 2
Mineral composition of three selected shale samples.

Depth, m	Quartz, %	K-feldspar, %	Plagioclase, %	Calcite, %	(Fe-) Dolomite, %	Dolomite, %	Siderite, %	Pyrite, %	Total Clay, %
2107.59	33.1	1.6	26.2	0.5	0	0	1.8	3	33.7
2088.99	31.8	0.2	25.7	0.6	0	0	0	6.1	35.6
2138.60	32.38	0.00	9.03	6.48	3.96	18.50	0.62	0.70	28.33

Table 3
Summary of the weight changes and hydrogen content changes of shale samples under imbibition and drying process.

Shale Sample Depth	Portion	Condition	Weight, g	NMR H, mg
2107.59 m	Oil	Native	18.246	65.446
		Imbibed	18.520	116.434
		Dried	18.352	87.842
	Brine	Native	20.290	63.940
		Imbibed	20.844	125.962
		Dried	20.347	74.054
2088.99 m	Oil	Native	41.686	115.172
		Imbibed	42.415	223.825
		Dried	41.945	164.300
	Brine	Native	26.885	72.103
		Imbibed	27.189	113.535
		Dried	26.801	58.997
2138.60 m	Oil	Native	21.175	63.707
		Imbibed	21.515	108.764
		Dried	21.181	65.948
	Brine	Native	21.620	62.460
		Imbibed	22.002	106.512
		Dried	21.442	44.419

Table 4
Summary of weight and hydrogen content changes of shale sample from 2017.59 m depth during imbibition and evaporation process.

Shale Sample Depth	Portion	Condition	Sample Weight, g	NMR H, mg
2107.59 m	Oil	Native	18.246	65.446
		2 days imbibed	18.505	109.184
		5 days imbibed	18.487	106.110
		14 days imbibed	18.515	113.772
		21 days imbibed	18.520	116.434
		2 h dried	18.461	105.004
		4 h dried	18.436	100.156
		10 h dried	18.420	97.384
		16 h dried	18.399	95.578
		22 h dried	18.364	88.838
		24 h dried	18.352	87.842
	Brine	Native	20.290	63.940
		2 days imbibed	20.646	104.216
		5 days imbibed	20.664	105.143
		14 days imbibed	20.702	109.151
		21 days imbibed	20.844	125.962
		2 h dried	20.692	112.321
		4 h dried	20.572	101.021
		10 h dried	20.495	87.652
		16 h dried	20.424	83.097
		22 h dried	20.363	73.590
		24 h dried	20.347	74.054

days, 14 days and 21 days. The NMR T_1-T_2 maps of the shale sample at different dried stages, 6 h, 10 h, 16 h and 24 h, are shown in Fig. 5. These T_1-T_2 maps clearly illustrate how water and oil moved during oil or brine imbibition process. The imbibed oil caused several highlighted zones and imbibed brine led to an obvious shiny zone. Imbibed brine increased the intensity of NMR signal as well as the T_2 value (shift to the right). After evaporating, the shift areas had a tendency to return to their initial position.

To understand the oil and water migrations, all NMR T_1-T_2 maps acquired from shale samples from 2088.99 m to 2138.60 m depth were divided into four regions corresponding to its various T_1 and T_2 distribution. The intensity of NMR signal in each region was already calibrated in hydrogen content unit, mg.

NMR T_1-T_2 maps of shale samples from 2088.99 m depth are shown in Fig. 6. Two portions of shale sample under native condition are basically identical in composition for the similar proportion and distribution of each region in T_1-T_2 maps, as shown in Fig. 6a and d. Therefore, the subsequent experiments in two portions of each shale sample are comparable. In the main, the strength of signal in all regions increased after imbibition process and decreased after evaporation. Oil imbibition caused an obvious increment in Region 3, as shown in Fig. 6b. By contrast, brine imbibition caused an increment in Region 2, as shown in Fig. 6e. Significantly, Region 1 and Region 4 slightly changed after the oil or brine imbibition. After evaporation, all regions, to a large extent, recovered to the original states as shown in Fig. 6c and f.

NMR T_1-T_2 maps of shale samples from 2138.60 m depth are shown in Fig. 7. The changes of NMR signals in four regions among different conditions in Fig. 7 are similar to Fig. 6, except for some differences in Region 3 between oil imbibed condition and native condition, as shown in Figs. 7b and 6b.

3.4. Capability of two shale samples to imbibe oil and brine

Table 5 compares the weight changes of two chunks of shale samples from 2088.99 m to 2138.60 m depth in the 60-h oil imbibition and brine imbibition. The shale sample from 2088.99 m gained more weight per unit mass in oil imbibition than brine imbibition. While the shale sample from 2138.60 m depth got a little bit more weight per unit mass in brine imbibition than oil imbibition.

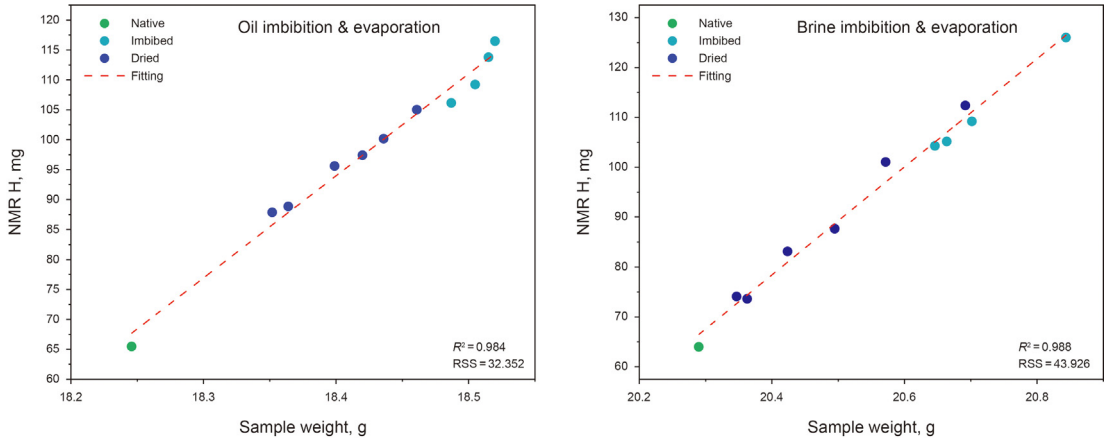

Fig. 3. Hydrogen contents measured by NMR 2D mapping of shale sample from 2017.59 m depth as a function of sample weight during imbibition and evaporation process. (a) Changes of oil portion in oil imbibition and evaporation. (b) Changes of brine portion in brine imbibition and evaporation.

4. Discussions

4.1. Consistence in hydrogen content and incremental weight during imbibition and evaporation

To a certain extent, change of hydrogen content is consistent with the incremental weight during imbibition and evaporation. But there are still gaps between NMR results and sample weight. Errors may come from the volatilization of imbibed liquid (shale sample can be heated while pulse transmitting) and the weight loss of shales (some slags may drop during imbibition and evaporation process because of the brittle nature of shales) during the NMR experiment. Besides error from samples, NMR analyzer is sensitive and error from signal noise should be considered as well. The

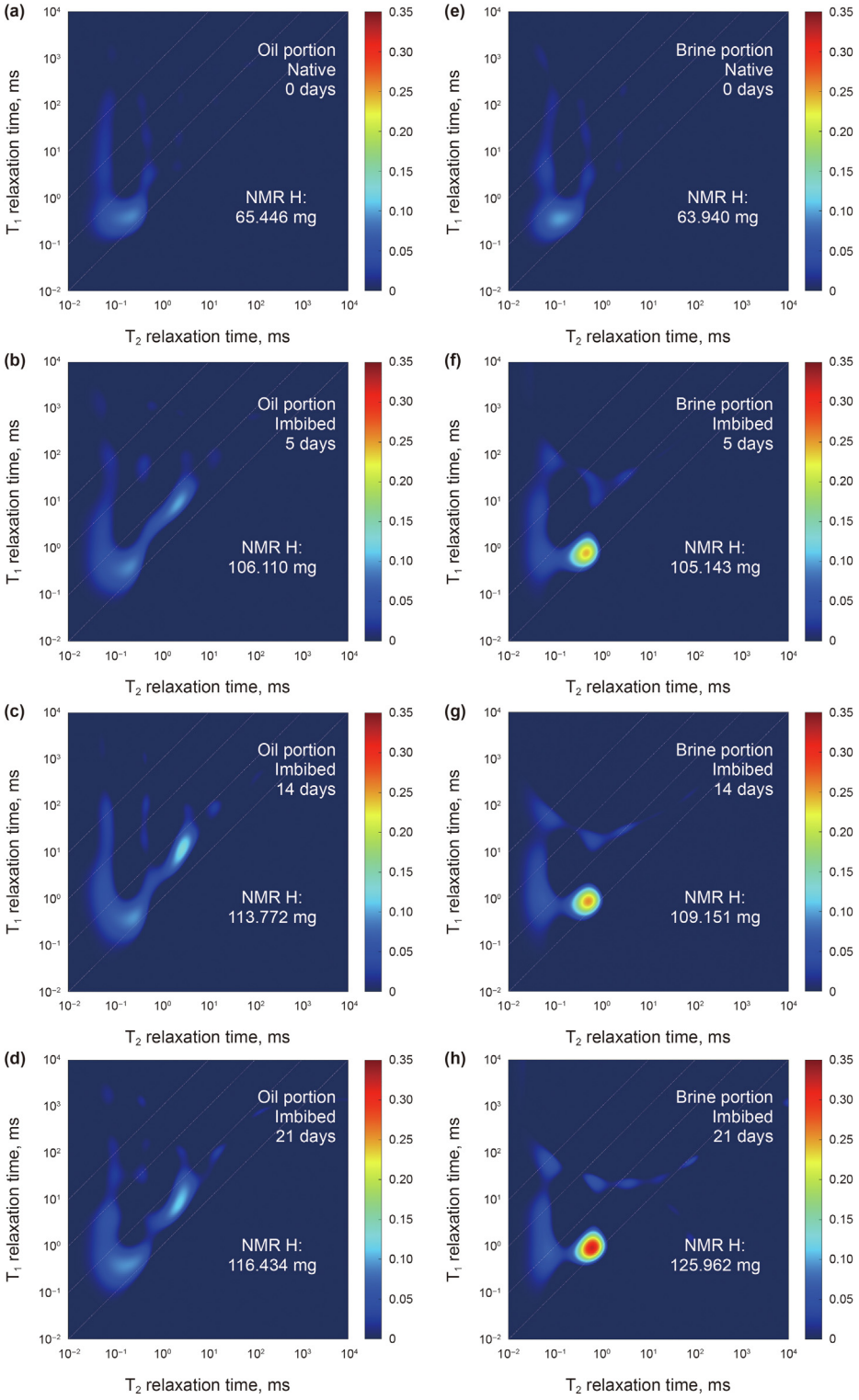

Fig. 4. NMR T_1-T_2 maps of the shale sample from 2107.59 m depth at different imbibed stages of 0 days, 5 days, 14 days and 21 days.

imperfect applicability of $CuSO_4$ solution to calibrate hydrogen content in shale samples can also result in some gaps between hydrogen content measured by NMR 2D mapping and its true value.

Although these gaps did exist, the relative changes measured by NMR 2D mapping are still enough to be convincing.

4.2. Deviations of hydrogen content in shale samples between dried condition and native condition

The NMR signals of three shale sample as native condition were not very low because these samples still had some liquid such as water or oil and organic matter in them before imbibition experiment.

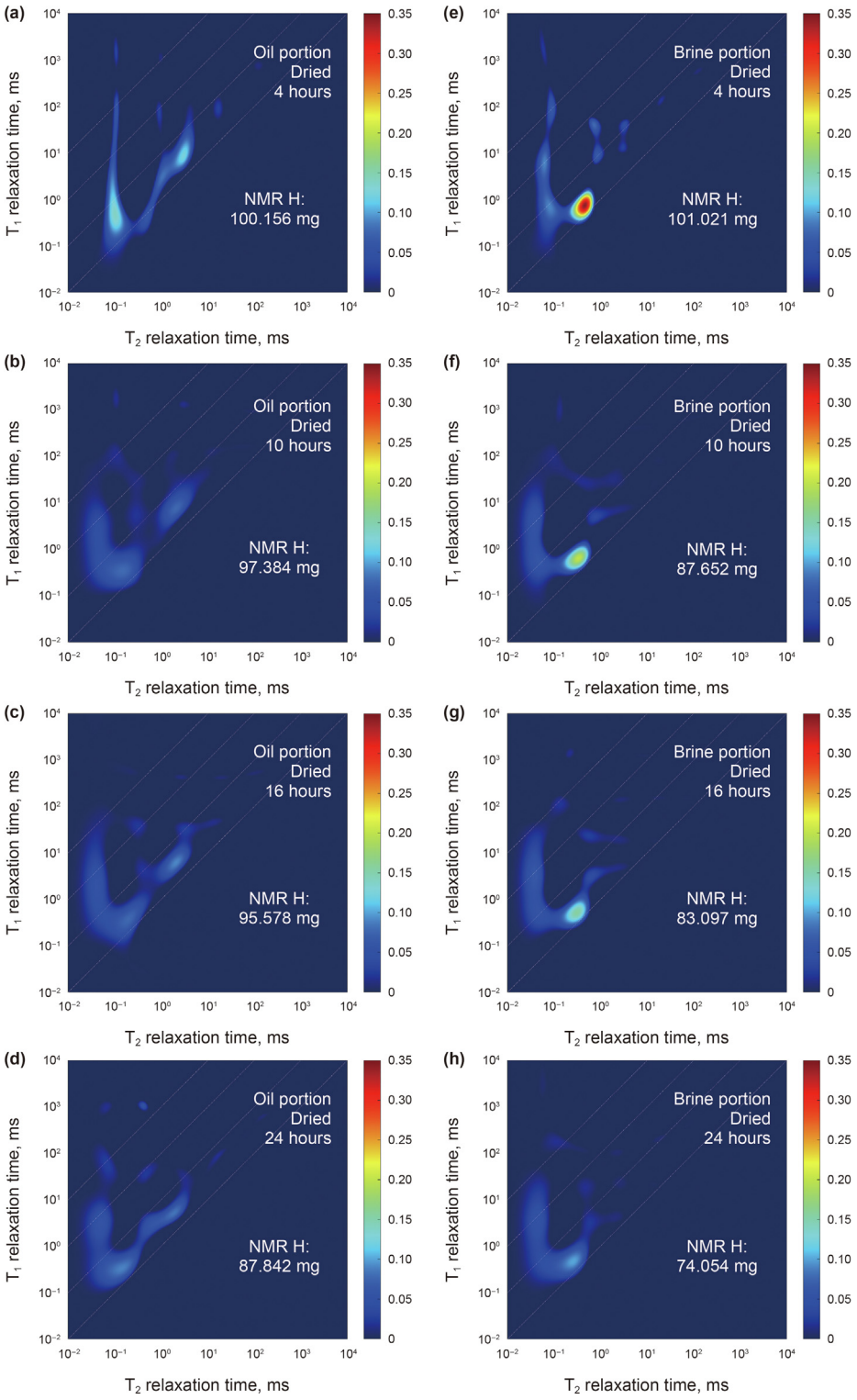

Fig. 5. NMR T_1-T_2 maps of the shale sample from 2107.59 m depth at different dried stages of 4 h, 10 h, 16 h and 24 h.

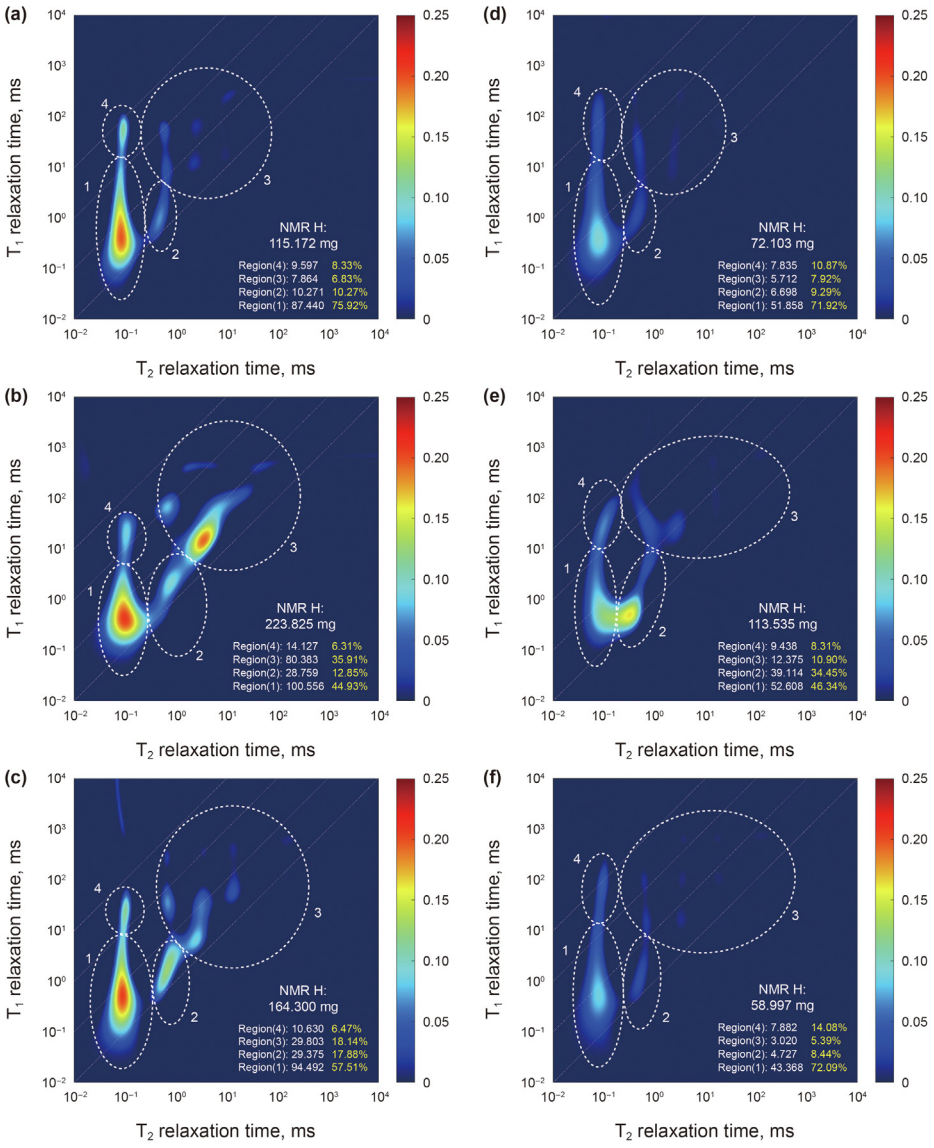

Shale sample depth	Portion	Status	NMR H, mg								
			Region 1		Region 2		Region 3		Region 4		All map
2138.60 m	Oil	Native	87.440	75.92%	10.271	10.27%	7.864	6.83%	9.597	8.33%	115.172
		Imbibed	100.556	44.93%	28.759	12.85%	80.383	36.91%	14.127	6.31%	223.825
		Dried	94.492	57.51%	29.375	17.88%	29.803	18.14%	10.63	6.47%	164.300
	Brine	Native	51.858	71.92%	6.698	9.29%	5.712	7.92%	7.835	10.87%	72.103
		Imbibed	52.608	46.34%	39.114	34.45%	12.375	10.90%	9.438	8.31%	113.535
		Dried	43.368	72.09%	4.727	8.44%	3.020	5.39%	7.882	14.08%	58.997

Fig. 6. NMR T_1-T_2 maps of two portions of shale samples from 2088.99 m depth at different stages. (a) Oil portion under native condition. (b) Oil portion under imbibed condition. (c) Oil portion under dried condition. (d) Brine portion under native condition. (e) Brine portion under imbibed condition. (f) Brine portion under dried condition.

For shale sample under three-week imbibition (shale sample from 2107.59 m depth), the positive deviation of hydrogen content between dried and native condition represents that the imbibed oil and water was not evaporated completely. It could be attribute to the low temperature of oven and short drying time.

For shale samples under 60-h imbibition (shale samples from 2088.99 m to 2138.60 m depth), the positive deviation of hydrogen content in oil portion between dried and native condition represents that the imbibed oil was not evaporated completely as well, as shown in Fig. 6a and c, Fig. 7a and c. As for water portion, the negative deviation shows that imbibed liquid was evaporated completely and even bound liquid, which existed in native condition was also lost, based on the differences of Region 2 between Fig. 6d and f, Fig. 7d and f.

The differences in hydrogen content of shale samples between three-week imbibition and 60-h imbibition may not only result from the volume of imbibed liquid, but also result from how water bounded. Of course, the water staying on surface is easier to dry out than that in internal pores. Pores structure, organic matter and clay in shales can also affect the evaporation, which also indicates that the wettability of pores in shales may lead to these differences. Moreover, the different properties of decane and brine should also be taken into consideration.

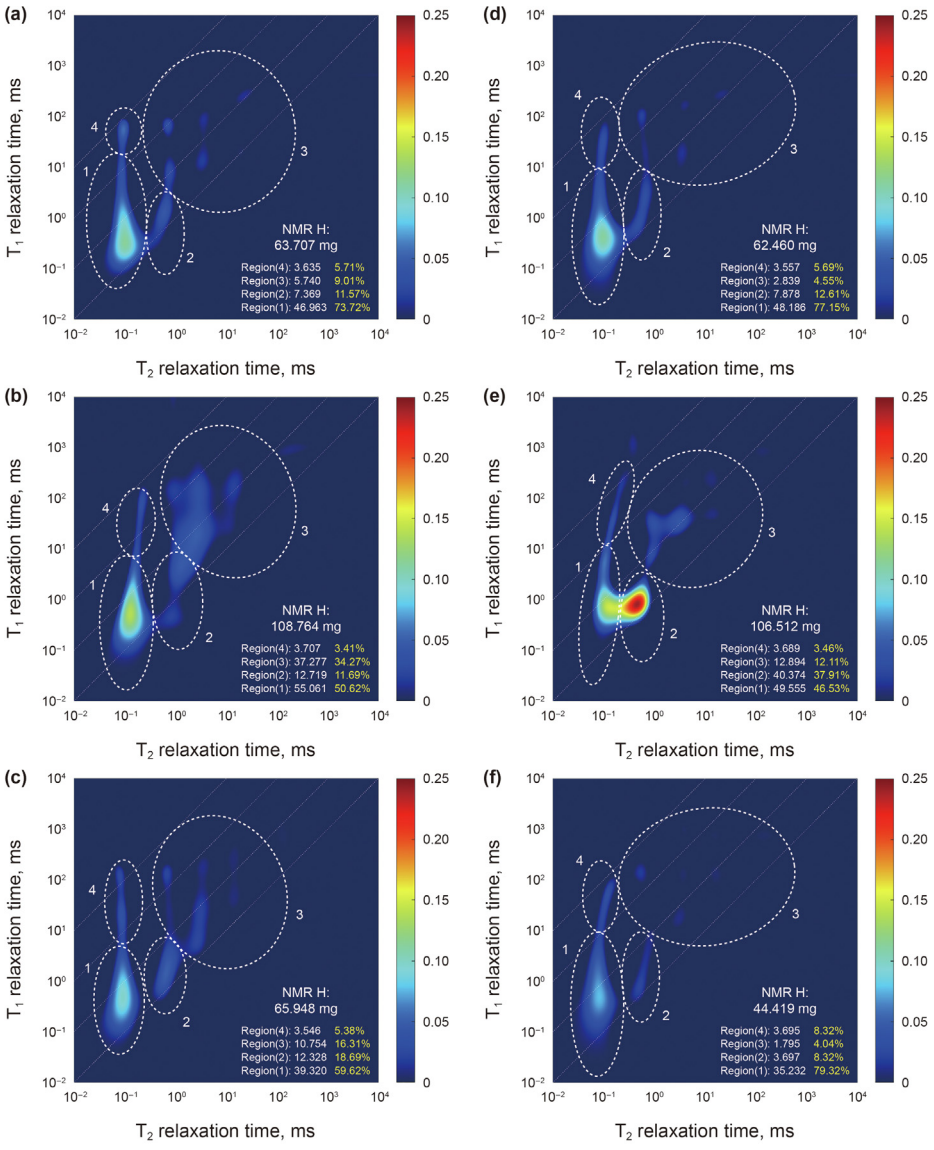

Shale sample depth	Portion	Status	NMR H, mg								
			Region 1		Region 2		Region 3		Region 4		All map
2138.60 m	Oil	Native	46.963	73.73%	7.369	11.57%	5.740	9.01%	3.635	5.71%	63.707
		Imbibed	55.061	50.62%	12.719	11.69%	37.277	34.27%	3.707	3.41%	108.764
		Dried	39.320	59.62%	12.328	18.69%	10.754	16.31%	3.546	5.38%	65.948
	Brine	Native	48.186	77.15%	7.878	12.61%	2.839	4.55%	3.557	5.69%	62.460
		Imbibed	49.555	46.53%	40.374	37.91%	12.894	12.11%	3.689	3.46%	106.512
		Dried	35.262	79.32%	3.697	8.32%	1.795	4.04%	3.695	8.32%	44.419

Fig. 7. NMR T_1-T_2 maps of two portions of shale samples from 2138.60 m depth at different stages. (a) Oil portion under native condition. (b) Oil portion under imbibed condition. (c) Oil portion under dried condition. (d) Brine portion under native condition. (e) Brine portion under imbibed condition, (f) Brine portion under dried condition.

Table 5
Capability of two shale samples to imbibe oil and brine in the early 60 h.

Shale Sample Depth	Portion	Imbibed ΔW/W[a]
2088.99 m	Oil	1.75%
	Brine	1.13%
2138.60 m	Oil	1.61%
	Brine	1.77%

[a] Imbibed ΔW/W means imbibed weight of unit mass of shale samples.

4.3. T_2 shift in water imbibition and evaporation

T_2 value became larger as the water content increased as shown in Fig. 4. There are two major reasons for T_2 shift in shales. One reason is that small pores are filled with water first and then bigger pores. In this case, T_2 can become longer with increased water imbibition, considering the molecules moving more freely in larger pores. The other reason is the presence of clay in the shale sample from 2107.59 m depth. The increase of moisture can make the clay

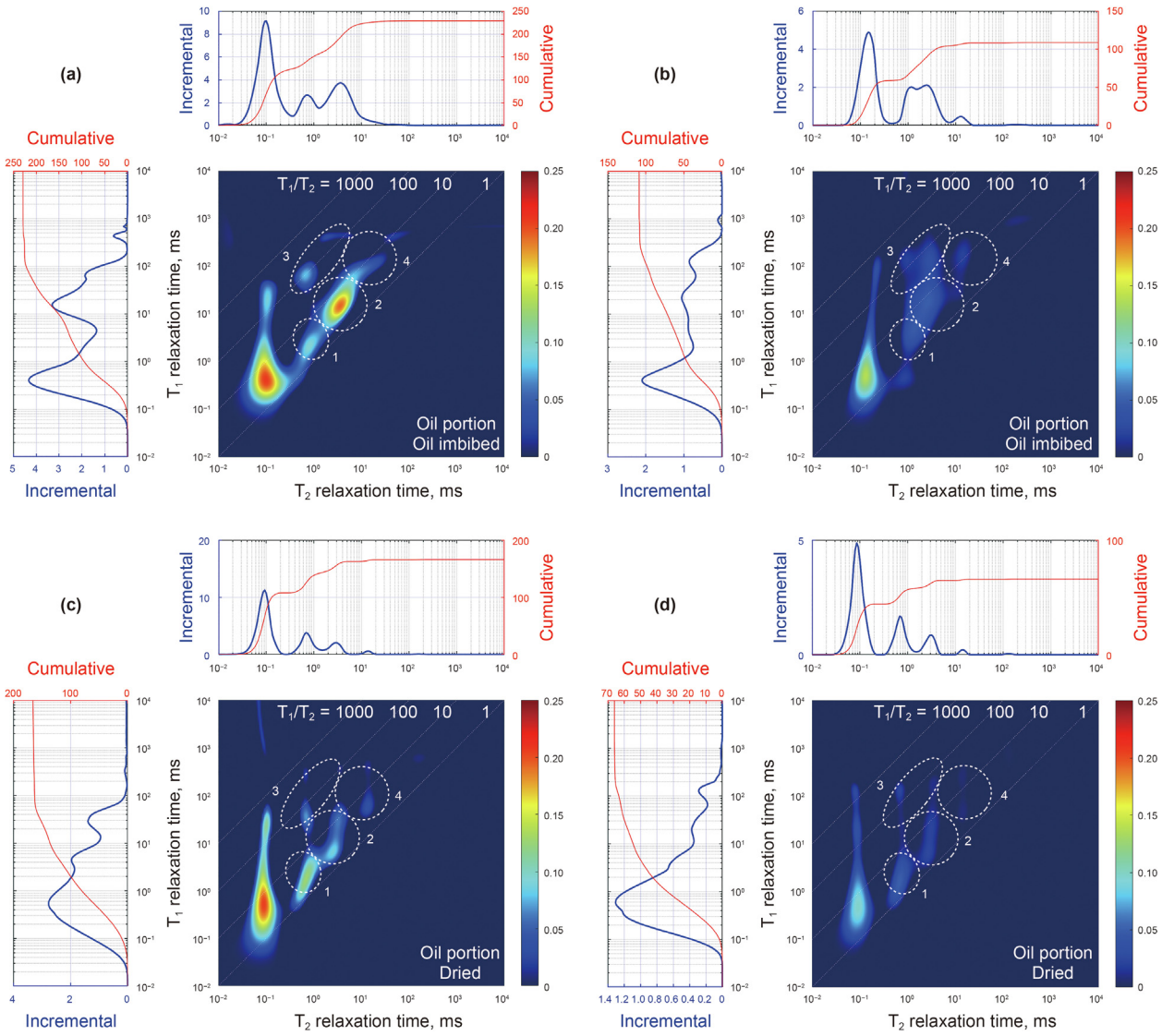

Fig. 8. NMR T_1-T_2 maps of shale sample under oil imbibed and dried condition. (a) Oil portion of shale sample from 2088.99 m depth under imbibed condition. (b) Oil portion of shale sample from 2138.60 m depth under imbibed condition. (c) Oil portion of shale sample from 2088.99 m depth under dried condition. (d) Oil portion of shale sample from 2138.60 m depth under dried condition.

swell, which can also cause T_2 to become longer (shifts to right) due to the properties of clay. Clay swelling can lead to the volume of inter-aggregate clay pores increase, further leading to the slower T_2 component, which represents discrete water phase in inter-aggregate clay pores (compared with the faster T_2 component as the characteristic of clay-bound water), become longer (Chitale et al., 2000).

4.4. Oil and water division in T_1-T_2 maps

According to the changes of signal strength in different regions in Figs. 6 and 7, it is easy to figure out that the Region 2 and Region 3 are closely related with imbibed water and oil, respectively. NMR signals in Region 1 and Region 4 are respectively from the bound water (or hydroxyl) and organic matter in rocks as their slightly changes considering the T_1 and T_2 features of tightly bound hydrogen. These results are consistent with general T_1-T_2 maps of shales (Khatibi et al., 2019).

Compared with brine imbibition, oil imbibition causes more complicated changes in NMR T_1-T_2 maps. To analyze more details of oil behaviors, 4 zones are circled both in NMR T_1-T_2 maps of shale samples from 2088.99 m to 2138.60 m depth in oil imbibed and dried condition, as shown in Fig. 8.

Obviously, Region 1 to 4 are all oil region according to differences among NMR T_1-T_2 maps of native, imbibed and dried samples. Region 1 to 3 have a similar lower T_1/T_2 ratio of 5 and from the highest T_2 to the lowest T_2, the order is Region 3, Region 2 and Region 1. Region 4 has a higher T_1/T_2 ratio of 100 with a lower intensity. After evaporation, most of the signals in Region 2 and Region 3 were lost, while most of the signals in Region 1 and Region 4 were still left. It indicates that oil in Region 2 and Region 3 with long T_2 time can move more freely than Region 1 and Region 4 with short T_2 time.

In addition, attention should be paid to the T_2 1D distribution (the upper curve in T_1-T_2 map in Fig. 8) that always be used in analysis of oil and water for conventional rocks. For our shales, T_2 1D distribution cannot differentiate these circled regions in Fig. 8 as a result of overlapping. That means T_2 1D distribution has its limits in distinguishing the oil, water, organic matter and bound water (or hydroxyl) for unconventional cores.

4.5. Influences of wettability, organic matter and magnetic minerals

These shale samples are all the mix-wet rocks according to the content of imbibed oil and brine in Table 5. It can also be seen from the geochemical characteristics and mineral composition such as high OSI value and clay content. Differences in oil region of two shale samples (shale samples from 2088.99 m to 2138.60 m depth) between oil imbibed condition and native condition (shown in Figs. 6b and 7b) may represent the different pore-size distribution or connectivity, and wettability between two chunks of shale samples from different depth.

Molecules of heavy or solid organics are less mobile, and their T_2 values are very short and T_1 values are relatively long leading to high T_1/T_2 ratios, i.e. the Region 4 on the map as shown in Figs. 6 and 7. Region 4 changed slightly during the imbibition and evaporation and Fig. 6 (shale sample from 2088.99 m depth) shows a little bit high value in Region 4 compared with Fig. 7 (shale sample from 2138.60 m depth), which is roughly consistent with the TOC content, as shown in Table 1.

Although there was a magnetic mineral component in these shale samples, the content was not high and ferromagnetic or paramagnetic substances didn't lead to the apparent decrease of T_2 value in T_1-T_2 maps. Therefore, the influences of magnetic minerals are supposed to be little in the 20 MHz NMR 2D mapping experiments.

5. Conclusions

20 MHz 2-D NMR relaxometry techniques play a key role in studying water and oil migrations of Chinese lacustrine Qingshankou shales from a qualitative and quantitative view. The hydrogen content calibrated by NMR signals of shales shows a good linear relationship with the weight increment in imbibition and evaporation process. NMR T_1-T_2 map can give a visual display of the content of various components such as water, oil, bound water and solid organic matter in shales based on their different T_1 and T_2 features. The differences between regions on T_1-T_2 maps show dynamic migrations of water and oil in pores during the imbibition and evaporation. According to imbibition experiments, water region is more concentrated along the diagonal line (T_1/T_2 ratio close to 1), while oil region has a more complex distribution with a broad range of T_1/T_2 ratio (T_1/T_2 5–100) that may be affected by other complicated properties such as pore-size distribution, connectivity, organic matter and wettability of shales. Compared with NMR T_1-T_2 map, T_2 1-D distribution may be limited because of partial overlapping of oil region, water region and organic region projections in T_1 direction. T_2 value can increase with the clay swelling, therefore water region shifts to right when water is imbibed and shifts to left after drying. Wettability of shale samples can also be illustrated according to the weight increment, and T_1-T_2 map changes in oil and brine imbibition to some extent. Influences of small amount of magnetic minerals in shales are supposed to be little in NMR 2D mapping experiments.

Acknowledgement

This project is supported by the Opening Fund of Key Laboratory of Continental Shale Accumulation and Development (Northeast Petroleum University, China) and the National Natural Science Foundation of China (Grant No. 51605089, Grant No. 41972156). We thank two labs' partners for their provision of shale samples, valuable scientific discussions and all their support and help in NMR experiments.

References

Baudin, F., Disnar, J.-R., Aboussou, A., Savignac, F., 2015. Guidelines for Rock–Eval analysis of recent marine sediments. Org. Geochem. 86, 71–80. https://doi.org/10.1016/j.orggeochem.2015.06.009.

Bloembergen, N., Purcell, E.M., Pound, R.V., 1948. Relaxation effects in nuclear magnetic resonance absorption. Phys. Rev. 73 (7), 679–712. https://doi.org/10.1103/PhysRev.73.679.

Blümich, B., Anferova, S., Pechnig, R., Pape, H., Arnold, J., Clauser, C., 2004. Mobile NMR for porosity analysis of drill core sections. J. Geophys. Eng. 1 (3), 177–180. https://doi.org/10.1088/1742-2132/1/3/001.

Chitale, D.V., Gardner, J., Sigal, R., June 2000. Significance of nmr T2 distributions from hydrated montmorillonites. In: SPWLA 41st Annual Logging Symposium. Dallas, Texas.

Coates, G.R., Xiao, L., Prammer, M.G., 1999. NMR Logging: Principles and Applications. Gulf Professional Publishing.

Deng, F., Xiong, C., Chen, S., Chen, G., Wang, M., Liu, H., et al., 2020. A method and device for online magnetic resonance multiphase flow detection. Petrol. Explor. Dev. 47 (4), 855–866. https://doi.org/10.1016/s1876-3804(20)60101-x.

Fan, Y.R., Liu, J.Y., Ge, X.M., et al., 2018. Permeability evaluation of tight sandstone based on dual T2 cutoff values measured by NMR. Chin. J. Geophys. 61 (4), 1628–1638. https://doi.org/10.6038/cjg2018L0037 (in Chinese).

Fleury, M., Romero-Sarmiento, M., 2016. Characterization of shales using T1–T2 NMR maps. J. Petrol. Sci. Eng. 137, 55–62. https://doi.org/10.1016/j.petrol.2015.11.006.

Gao, F., Song, Y., Li, Z., Xiong, F., Chen, L., Zhang, X., et al., 2018. Quantitative characterization of pore connectivity using NMR and MIP: a case study of the Wangyinpu and Guanyintang shales in the Xiuwu basin, Southern China. Int. J. Coal Geol. 197, 53–65. https://doi.org/10.1016/j.coal.2018.07.007.

Godefroy, S., Korb, J.P., Fleury, M., Bryant, R.G., 2001. Surface nuclear magnetic relaxation and dynamics of water and oil in macroporous media. Phys. Rev. E 64 (2). https://doi.org/10.1103/PhysRevE.64.021605.

Guo, J.C., Zhou, H.Y., Zeng, J., Wang, K.J., Lai, J., Liu, Y.X., 2020. Advances in low-field nuclear magnetic resonance (NMR) technologies applied for characterization of pore space inside rocks: a critical review. Petrol. Sci. 17 (5), 1281–1297. https://doi.org/10.1007/s12182-020-00488-0.

Khatibi, S., Ostadhassan, M., Xie, Z.H., Gentzis, T., Bubach, B., Gan, Z., et al., 2019. NMR relaxometry a new approach to detect geochemical properties of organic matter in tight shales. Fuel 235, 167–177. https://doi.org/10.1016/j.fuel.2018.07.100.

Kleinberg, R.L., Kenyon, W.E., Mitra, P.P., 1994. Mechanism of nmr relaxation of fluids in rock. J. Magn. Reson. 108 (2), 206–214. https://doi.org/10.1006/jmra.1994.1112.

Korb, J.P., 2018. Multiscale nuclear magnetic relaxation dispersion of complex liquids in bulk and confinement. Prog. Nucl. Magn. Reson. Spectrosc. 104, 12–55. https://doi.org/10.1016/j.pnmrs.2017.11.001.

Korb, J.P., Nicot, B., Louis-Joseph, A., Bubici, S., Ferrante, G., 2014. Dynamics and wettability of oil and water in oil shales. J. Phys. Chem. C 118 (40), 23212–23218. https://doi.org/10.1021/jp508659e.

Liao, G.Z., Chen, W.L., Zong, F.R., Deng, F., Liu, H.B., Wu, B.S., et al., 2021. NMR fluid analyzer applying to petroleum industry. Petrol. Sci. 18 (1), 54–91. https://doi.org/10.1007/s12182-020-00529-8.

Liang, C., Xiao, L.Z., Zhou, C.C., et al., 2019. Nuclear magnetic resonance characterizes rock wettability: preliminary experimental results. Chin. J. Geophys. 62 (11), 4472–4481. https://doi.org/10.6038/cjg2019M0266 (in Chinese).

Liu, B., Bai, L., Chi, Y., Jia, R., Fu, X., Yang, L., 2019a. Geochemical characterization and quantitative evaluation of shale oil reservoir by two-dimensional nuclear magnetic resonance and quantitative grain fluorescence on extract: a case study from the Qingshankou Formation in Southern Songliao Basin, northeast China. Mar. Petrol. Geol. 109, 561–573. https://doi.org/10.1016/j.marpetgeo.2019.06.046.

Liu, B., Wang, H., Fu, X., Bai, Y., Bai, L., Jia, M., et al., 2019b. Lithofacies and depositional setting of a highly prospective lacustrine shale oil succession from the Upper Cretaceous Qingshankou Formation in the Gulong sag, northern Songliao Basin, northeast China. AAPG (Am. Assoc. Pet. Geol.) Bull. 103, 405–432. https://doi.org/10.1306/08031817416.

Liu, B., Yang, Y., Li, J., Chi, Y., Li, J., Fu, X., 2020. Stress sensitivity of tight reservoirs and its effect on oil saturation: a case study of Lower Cretaceous tight clastic reservoirs in the Hailar Basin, Northeast China. J. Petrol. Sci. Eng. 184. https://doi.org/10.1016/j.petrol.2019.106484.

Liu, C.L., Wang, Z.L., Guo, Z.Q., Hong, W.Y., Dun, C., Zhang, X., et al., 2017. Enrichment and distribution of shale oil in the cretaceous Qingshankou Formation, Songliao Basin, northeast China. Mar. Petrol. Geol. 86, 751–770. https://doi.org/10.1016/j.marpetgeo.2017.06.034.

Liu, Y., Yao, Y., Liu, D., Zheng, S., Sun, G., Chang, Y., 2018. Shale pore size classification: an NMR fluid typing method. Mar. Petrol. Geol. 96, 591–601. https://doi.org/10.1016/j.marpetgeo.2018.05.014.

McPhee, C., Reed, J., Zubizarreta, I., 2015. Chapter 5 - routine core analysis. Dev. Petrol. Sci. 181–268.

Ramia, M.E., Martín, C.A., 2016. Nuclear magnetic resonance relaxation studies in shale. Appl. Magn. Reson. 47 (12), 1323–1337. https://doi.org/10.1007/s00723-016-0834-0.

Shi, J.F., Deng, F., Xiao, L.Z., Liu, H.B., Ma, F.Q., Wang, M.Y., et al., 2019. A proposed NMR solution for multi-phase flow fluid detection. Petrol. Sci. 16 (5), 1148–1158. https://doi.org/10.1007/s12182-019-00367-3.

Testamanti, M.N., Rezaee, R., 2017. Determination of NMR T2 cut-off for clay bound water in shales: a case study of Carynginia Formation, Perth Basin, Western Australia. J. Petrol. Sci. Eng. 149, 497–503. https://doi.org/10.1016/j.petrol.2016.10.066.

Tian, Z., 2021. NMR diffusional coupling of multiple-scale porous rock and its detection Chinese. J. Geophys. 64 (3), 1119–1130. https://doi.org/10.6038/cjg2021O0081 (in Chinese).

Wang, F.Y., Yang, K., Zai, Y., 2020. Multifractal characteristics of shale and tight sandstone pore structures with nitrogen adsorption and nuclear magnetic resonance. Petrol. Sci. 17 (5), 1209–1220. https://doi.org/10.1007/s12182-020-00494-2.

Xie, R.H., Xiao, L.Z., 2011. Advanced fluid-typing methods for NMR logging. Petrol. Sci. 8, 163–169. https://doi.org/10.1007/s12182-011-0130-4.

Xie, Z.H., Gan, Z., June 2018. Value of 20Mhz NMR core analysis for unconventional mudstones. In: SPWLA 59th Annual Logging Symposium. London, UK.

Xie, Z.H., Gan, Z., June 2019. Investigation of physical properties of hydrocarbons in unconventional mudstones using two-dimensional NMR relaxometry. In: SPWLA 60th Annual Logging Symposium. The Woodlands, Texas, USA. https://doi.org/10.30632/T60ALS-2019_ZZZ.

Zhong, J., Yan, R., Zhang, H., Feng, Y., Li, N., Liu, X., 2020. A decomposition method of nuclear magnetic resonance T2 spectrum for identifying fluid properties. Petrol. Explor. Dev. 47 (4), 740–752. https://doi.org/10.1016/s1876-3804(20)60089-1.